Atmos. Chem. Phys. Discuss., https://doi.org/10.5194/acp-2018-1190
Manuscript under review for journal Atmos. Chem. Phys.
Discussion started: 7 January 2019
© Author(s) 2019. CC BY 4.0 License.

Atmospheric Chemistry and Physics Discussions

Seasonal features and origins of carbonaceous aerosols at Syowa Station, Antarctica

Keiichiro Hara[1], Kengo Sudo[2], Takato Ohnishi[2], Kazuo Osada[2], Masanori Yabuki[3], Masataka Shiobara[4], Takashi Yamanouchi[4]

[1] Department of Earth System Science, Faculty of Science, Fukuoka University, Fukuoka, 814-0180, Japan
[2] Graduate School of Environmental Studies, Nagoya University, Nagoya, 464-8601, Japan
[3] Research Institute for Sustainable Humanosphere, Kyoto University, Kyoto, 611-0011, Japan
[4] National Institute of Polar Research, Tokyo, 190-0014, Japan

Correspondence to: Keiichiro Hara (harakei@fukuoka-u.ac.jp)

Abstract. We measured equivalent black carbon (EBC) concentrations at Syowa Station, Antarctica from February 2005 to characterize seasonal features of EBC concentrations and their origins, and to monitor long-range transport of aerosols from mid-latitudes to the Antarctic coast. Results show that EBC concentrations were below the detection limit (0.2 ng m^{-3}) to 63.8 ng m^{-3} at Syowa Station (median, 1.8 ng m^{-3}; mean, 2.7 ng m^{-3} during the measurement period). Although seasonal features and year-to-year variations of EBC concentrations were observed, no long-term trend of EBC concentrations was clear during our measurement period. Seasonal features of EBC concentrations showed a spring maximum during September–October at Syowa Station. The absorption Ångström exponent (AAE) was 0.5–1.0 during April–October; it reached its maximum values (1.0–1.5) during summer. The AAE features imply that EBC was mixed internally in the Antarctic troposphere and that organic aerosols engendered high AAE in the summer. To elucidate EBC transport processes, origins, and the potential source area (PSA), we compared EBC data to backward trajectory analysis and model simulation. Results show that EBC might be transported directly to Syowa Station from mid-latitudes mainly via the boundary layer and the lower free troposphere. Some BC was transported to Antarctic regions via the upper free troposphere. Biomass burning in South America and southern Africa is the most dominant PSA for BC transported to Syowa Station. Fossil fuel combustion in South America and southern Africa also have important contributions.

1 Introduction

Carbonaceous aerosols are major aerosol components of the troposphere. In general, carbonaceous aerosols contain organic compounds and particulate graphite (Gelencsér, 2004). Various terms such as elemental carbon (EC), black carbon (BC), and soot are used to describe carbonaceous particles. As defined by Novakov (1984), BC comprises particulate graphitic particles. Because of their strong optical absorption, BC has been a concern for atmospheric radiation budgets and climate effects (e.g., Bond et al., 2013, references therein). In addition to BC, mineral particles containing iron oxides (e.g., hematite and magnetite) and some organic aerosols (e.g., brown carbon (BrC)) have light absorption in visible and ultraviolet (UV) spectral bands (Bond et al., 2013, references therein; Moteki et al., 2017). Furthermore, BC can alter surface albedo after deposition onto snow surfaces in polar regions (e.g., Flanner et al., 2007; Aoki et al., 2011; Hadley and Kirchstetter, 2012; Bond et al., 2013). In Antarctic regions, BC effects on radiation budgets are regarded as negligible because of low BC concentration (e.g., Bodhaine, 1995; Weller et al., 2013).

Atmospheric BC is released directly from incomplete combustion processes. Antarctic regions are isolated from large combustion sources related to human activities at low latitudes and mid-latitudes. Therefore, local origins of BC in the Antarctic area are limited to (1) human activity at research stations, (2) usage of snow vehicles for travel, (3) operations of airplanes and research vessels during summer, and (4) ship-borne tourism mainly on the Antarctic Peninsula (Shirasat and Graf, 2009; Graf et al., 2010). Although local contamination from these sources can engender temporarily high BC

© Author(s) 2019. CC BY 4.0 License.

concentrations (e.g., Wolff and Cachier, 1998; Hansen et al., 2001; Hagler et al., 2008), the BC source strength is likely to be negligible or only slight throughout Antarctic regions. Indeed, earlier work has shown that BC concentrations are lower at higher latitudes (Wolff and Cachier, 1998; Weller et al., 2013). Because of the low BC source strength in Antarctic regions, BC must be supplied from outside of Antarctica, i.e. long-range transport, to maintain the background BC level and its seasonal features in the Antarctic atmosphere. In other words, BC in the Antarctic atmosphere is useful as a tracer of atmospheric substances derived from combustion processes occurring at mid-latitudes and low latitudes.

Earlier studies (Wolff and Cachier, 1998; Weller et al., 2013) have pointed out the likelihood that BC in the Antarctic atmosphere originates from biomass burning. Additionally, BC is transported directly from South America (Fiebig et al., 2009; Hara et al., 2010) and from southern Africa (Hara et al., 2010) by poleward flow associated with cyclone activity in the Southern Ocean. Additionally, Weller et al. (2013) and Perreira et al. (2006) demonstrated that BC at Neumayer and Ferraz is supplied from biomass burning in South America. Levoglucosan, as a tracer of biomass burning, was detected in aerosols and snow taken in the Antarctica (Gambaro et al., 2008, Hu et al., 2013; Zangrando et al., 2016). Therefore, the BC must be transported from areas where the biomass burning occurred. In fact, BC records for the past 150 years in the Antarctic ice core show association with ENSO (El Niño-Southern Oscillation) and show variation in grassland and biofuel BC emissions (Bisiaux et al., 2012). Furthermore, high correlation between BC and NH_4^+ in the Antarctic ice core indicates BC and NH_4^+ from primary sources of biomass burning (Pasteris et al., 2014). Certainly, BC measurements taken during a few decades at Neumayer indicate an unclear long-term trend of BC concentrations, although a slight decreasing trend can be observed in summer (Weller et al., 2013).

In contrast to the Arctic atmosphere, anthropogenic effects have been reported as negligible for aerosols in the Antarctic atmosphere (e.g., Weller et al., 2011, 2013). However, some anthropogenic metals such as Pb have been found in snow and ice cores in Antarctic regions (Planchon et al., 2002; Vallelonga et al., 2002). Considering that biomass burning occurs on the ground in forests and grasslands, anthropogenic BC (derived mainly from fossil fuel combustion) can be transported to Antarctica. With recent economic development of countries of the Southern Hemisphere, the contributions of anthropogenic BC should not be ignored. They must be assessed. Nevertheless, the contributions of biomass burning and anthropogenic processes to BC concentrations in the Antarctic troposphere and their potential source area (PSA) have been neither quantitatively analyzed nor discussed in the relevant literature.

To elucidate transport from the low latitudes and mid-latitudes to the Antarctic regions, earlier studies have been conducted to analyze and assess PSA of mineral particles based on Nd/Sr isotope ratios (Smith et al., 2003; Delmonte et al., 2004, 2008; Bory et al., 2010; Valleloga et al., 2010; Aarons et al., 2016), Pb isotope ratios (De Deckker et al., 2010; Gilli et al., 2016), rare earth element patterns (Gabrielli et al., 2010; Valleloga et al., 2010; Wegner et al., 2012, Aarons et al., 2016), and trajectory/models (Perreira et al., 2004; Gasso et al., 2010; Li et al., 2008; Krinner et al., 2010; Albani et al., 2010; Neff and Bertler, 2015). From the aspect of mineral particles transported into the Antarctica, South America (mostly Patagonia) has been identified as the most dominant PSA, whereas Australia shows minor PSA. Although our earlier study showed direct transport of BC from southern Africa (Hara et al., 2010), southern Africa must be regarded as an unimportant PSA of mineral particles (e.g., Neff and Bertler, 2015). One must consider some differences between BC and minerals when evaluating this discrepancy: (1) geographical locations of PSA, (2) seasonality of source strength, and (3) size of aerosol particles containing BC and minerals. Mineral dusts comprise many elements, especially metals. Therefore, as described above, approaches of many kinds based on elemental information are available. However, similar procedures show difficulty in identifying BC origins because major BC component is graphite. Here, we attempt to combine BC measurements with backward trajectory

© Author(s) 2019. CC BY 4.0 License.

and model simulation. The present study was conducted to elucidate BC origins and PSA and to characterize BC concentrations and their seasonal features at Syowa Station, Antarctica located in the Indian Ocean sector.

2. Measurements and analysis

2.1 Aerosol measurements at Syowa Station, Antarctica

Aerosol measurements were conducted as a part of the Japanese Antarctic Expedition (JARE) at Syowa Station, Antarctica (69°00′S, 39°35′E), located as presented in Fig. 1. To Syowa, the icebreaker Shirase approaches every summer (mainly end-December – early February) for the transportation of fuel and materials for wintering operations and scientific activity. Some airplanes and helicopters operate occasionally during summer and not during other seasons. In contrast to the situation on the Antarctic Peninsula, ship-borne tourism was not done off Syowa during our measurements because of the station's distance from the other continents and the long distance between Syowa and the sea-ice margin (ca. 100 km even in summer). The BC concentrations were measured using a multi-wavelength aethalometer (AE31; Magee Scientific) from February 2005, although the aethalometer measurements stopped from January 2007 until January 2008 because of instrument trouble. The wavelengths of light sources in the aethalometer were 370, 470, 520, 590, 660, 880, and 950 nm. The aethalometer was operated in a clean air observatory located on the windward side of prevailing winds, ca. 400 m distant from the main area of Syowa, where a diesel power station was operating. The aethalometer operated under the following conditions: flow rate (ca. 9 L min^{-1} in 2005–2006 and ca. 11 L min^{-1} in 2008–present), data record resolution of 15 min, and spot change every 24 hr. For this study, we used a high-sensitivity AE31 instrument. The area of a circular spot to accumulate aerosols on the filter tape was 60.3 ± 1 mm^2. When winds come from the main area of the station, aerosol data can be contaminated considerably. Before data analysis and discussion, BC data were screened using wind data (direction and speed) provided from the Japan Meteorological Agency and using condensation nuclei concentrations obtained from JARE aerosol monitoring data. The data screening procedures were conducted in accordance with descriptions presented by Hara et al. (2010).

In an aethalometer, BC concentrations are measured by light attenuation resulting from optical absorption of BC collected on the filter tape. As earlier works have suggested (e.g., Weingartner et al., 2003; Bond et al., 2013), the filter-based BC measurements have scattering and shadowing effects that can engender error of BC measurements. Therefore, we used Weingartner's procedures for this study to correct BC concentrations (Weingartner et al., 2003; Supplementary). Light attenuation and optical attenuation coefficients in UV and visible ranges can be influenced greatly by optical absorption of organics and mineral dusts (e.g., Bond et al., 2013). Therefore, in this study, we used attenuation data in IR channel (λ = 880 nm) to estimate the BC concentrations. As reported by Bond et al. (2013), we use the term of equivalent BC (EBC) for the corrected mass BC concentrations and the measured BC concentrations using filter-base optical techniques in previous works, hereinafter. The detection limit of EBC in the aethalometer depends on the optical signal to noise ratio. We checked the optical signal to noise ratios of aerosol-free conditions in our measurement conditions. The detection limit was estimated as 0.2 ng m^{-3} in the IR channel under our measurement conditions (Δt = 120 min and flow rate, 10 L min^{-1}).

We use a multi-wavelength aethalometer for BC measurements. Therefore, the absorption Ångström exponent (AAE) was estimated in this study. The values of AAE can be represented as

$$C_{abs}(\lambda) = b_{abs}\lambda^{-AAE}, \quad (1),$$

where C_{abs}, and b_{abs} represent the optical absorption cross section at the λ (wavelength) and optical absorption coefficient. First, b_{abs} or b_{ATN} (optical attenuation coefficient) must be known to estimate AAE (Supplementary). Then, we estimated AAE in

© Author(s) 2019. CC BY 4.0 License.

UV–IR range (370–950 nm) and the visible (Vis)–IR range (590–950 nm) to understand impact of organics and EBC onto optical absorption properties.

2.2 Analysis of air mass origins

In this study, the 120-hr backward trajectory was computed to elucidate the transport pathway and origins of air masses transported to Syowa. The backward trajectory was calculated using the model vertical velocity mode in the NOAA-HYSPLIT model with meteorological data of NCEP reanalysis (Stein et al., 2015). The initial point was at an altitude of 500 m above ground level over Syowa, Antarctica. For comparison between BC concentrations and the air mass history, the backward trajectory was calculated every hour from January 2005 through December 2016 in this study.

2.3 CHASER (MIROC-ESM) Model

The CHASER model (Sudo et al., 2002; Sudo and Akimoto, 2007), developed mainly at Nagoya University and the Japan Agency for Marine-Earth Science and Technology (JAMSTEC), is a coupled CCM, simulating atmospheric chemistry and aerosols. Aerosols are examined by the SPRINTARS module (Takemura et al., 2005). It has been developed also in the framework of the MIROC Earth System Model, MIROC-ESM-CHEM (Watanabe et al., 2011). CHASER simulates details of chemistry in the troposphere and stratosphere with an online aerosol simulation including the production of particulate nitrate and secondary organic aerosols. As a standard configuration, the model's horizontal resolution is selected as T42 (2.8° × 2.8°), with 57 layers extending vertically from the surface up to about 55 km altitude. Regarding the overall model structure, CHASER is fully coupled with the climate model core MIROC, permitting atmospheric constituents (both gases and aerosols) to interact radiatively and hydrologically with meteorological fields in the model. The chemistry component of CHASER considers the O_x-NO_x-HO_x-CH_4-CO chemical system with oxidation of non-methane volatile organic carbons (NMVOCs), halogen chemistry, and the NH_x-SO_x-NO_3 system. In all, 96 chemical species and 287 chemical reactions are considered. In the model, primary NMVOCs include C_2H_6, C_2H_4, C_3H_8, C_3H_6, C_4H_{10}, acetone, methanol, and biogenic NMVOCs (isoprene, terpenes). In this study, CHASER uses interannually constant anthropogenic emissions (EDGAR-HTAP2-2008, http://edgar.jrc.ec.europa.eu/htap_v2/) with the biomass burning emission dataset (MACC reanalysis). The model was nudged to the NCEP FNL ds083 (u, v, T) and HadiSST/ICE (2000–2017).

The aerosol component of CHASER considers BC tracers of two types: hydrophobic BC (in external mixture) and hydrophilic BC (internally mixed with water-soluble species such as organics or SO_4^{2-}). In the latest model version, the aging process of BC in which hydrophobic BC is converted gradually to hydrophilic is simulated considering the condensation of sulfuric acid (H_2SO_4) and semi-volatile organic carbons onto the BC surface, and coagulation of BC with water-soluble particles (organics, SO_4^{2-}, etc.). The current model configuration calculates BC aging with time constants of less than one day in the PBLs, and a few days or weeks in the free troposphere depending on the abundances in SO_2, volatile organic carbons, and water-soluble aerosols.

For this study, a tagged BC tracer simulation is newly introduced into CHASER for estimating the respective contributions from different regions and types of emission to the long-range transport of BC. The tagged BC simulation, performed basically in the same framework of the tagged O_3 simulation developed by Sudo and Akimoto (2007), separates the globe into 15 regions as presented in Fig. 2 and calculates transport and deposition of BC emitted from the regions as distinct tracers. For the individual BC tracers, we also discriminate different emission sectors: (1) biomass burning, (2) fossil-fuel combustion, and (3) others (such as cocking and open burning). The tagged BC emissions are first injected into the atmosphere as hydrophobic BC (in external mixture). They then undergo aging processes to be converted to hydrophilic BC as described above. To avoid confusion of the term (e.g., EBC), we use the term of model-BC for the simulated mass BC concentrations hereinafter.

Atmos. Chem. Phys. Discuss., https://doi.org/10.5194/acp-2018-1190
Manuscript under review for journal Atmos. Chem. Phys.
Discussion started: 7 January 2019
© Author(s) 2019. CC BY 4.0 License.

Atmospheric Chemistry and Physics Discussions

3. Results and Discussion

3.1 Variations of EBC and AAE at Syowa Station, Antarctica

Figure 3 depicts seasonal features of EBC concentrations at Syowa Station, Antarctica from February 2005 through December 2016. In this study, median EBC concentrations are used for discussion, because the mean EBC concentrations can be overestimated relative to ambient EBC concentrations without local contamination when the unfilterable data derived from local contamination were present in our data screening procedures. Daily median EBC concentrations ranged from below the detection limit (<0.2 ng m^{-3}) to 63.8 ng m^{-3} during the measurement period. Frequent, median, and mean concentrations were, respectively, 1.1, 1.8, and 2.7 ng m^{-3}. In addition, the distributions of EBC concentrations were approximated by lognormal distributions (R^2= 0.9983) as

$$\mathrm{F}[EBC] = ae^{0.5\left(\frac{ln(EBC-EBC_0)}{b}\right)^2}, \quad (6),$$

where a, b, EBC_0 respectively stand for 529.75, 0.7270, and 1.12. The long-term trend of EBC was not clear at Syowa during our measurements (2005–2016), although a decreasing trend of EBC concentrations in summer was found at Neumayer (Weller et al., 2013). The EBC concentrations were similar to the EBC concentrations measured at coastal stations such as Halley and Neumayer (Wolff and Cahier, 1998; Weller et al., 2013). In contrast, EBC concentrations at Ferraz, Maitri, and Larsemann Hills were higher than those at Syowa (Pereira et al., 2006; Chaubey et al., 2010). Air masses at Ferraz were transported frequently from South America (Pereira et al., 2004), so that the long-range transport from South America might engender higher EBC concentrations at Ferraz than those in the other Antarctic coasts. The EBC concentrations at Maitri and Larsemann Hills during summer were markedly higher than those at Syowa and Neumayer. Considering the geographical locations of these stations as presented in Fig. 1, the high EBC concentrations at Maitri and Larsemann Hills might result from local contamination by human activity, as pointed out by Weller et al. (2013). Therefore, we concluded that EBC concentrations observed at Syowa corresponded to the EBC concentrations at the Antarctic coasts in the Indian Ocean sector.

Measurements of EBC concentrations exhibited clear seasonal features at Syowa with maximum (median, 3.1 ng m^{-3}) in August–November and minimum (1.3 ng m^{-3}) in January and February–April (Figs. 3a, 3c). Moreover, EBC concentrations at Syowa started increasing gradually in June and July. The spring maximum was observed also at Halley, Neumayer, and South Pole (Bodhaine, 1995; Wolff and Cachier, 1998; Weller et al., 2013). EBC measurements at Ferraz on the Antarctic Peninsula showed high EBC concentrations in September–January (Pereira et al., 2006). The spring maximum was found at all stations (Neumayer, Halley, and South Pole) with wintering EBC measurements. Therefore, this cannot be explained by local phenomena. Consequently, the spring EBC maximum might occur on the scale of the entire Antarctic region. Moreover, the spring EBC maximum appeared in a slightly earlier month at Syowa than in the periods examined at the other stations such as Neumayer. In addition to the spring maximum, a second maximum of EBC concentrations was found in summer (February – March/April) at Neumayer (Weller et al., 2013) and Ferraz (Pereira et al., 2006). However, the second EBC maximum was not identified clearly at Syowa. As pointed out by earlier studies (e.g., Wolff and Cachier, 1998; Fiebig et al., 2009; Hara et al., 2010; Weller et al., 2013), biomass burning has been regarded as having dominant origins of EBC in the Antarctic troposphere. Biomass burning in the Southern Hemisphere occurs in Africa, South America, Australia, and Indonesia (Edwards et al., 2006a, 2006b; Ito et al., 2007; Giglio et al., 2013). The burned area in each PSA increased drastically during July–September in Africa, August–October in South America, and September–November in Australia (Giglio et al., 2013). Considering that land-origin species such as EBC and mineral dusts can outflow eastwardly to the Southern Ocean because of cyclone activity and movement (e.g., Edwards et al., 2006a; Fiebig et al., 2009; Hara et al., 2010), the contribution of biomass burning from each PSA likely depends on the geographical locations of the respective coastal stations. For example, direct

© Author(s) 2019. CC BY 4.0 License.

transport from southern Africa might occur rarely at Neumayer and Halley, although direct transport was observed at Syowa (Hara et al., 2010). Therefore, the difference of the month in the spring EBC maximum at the Antarctic coasts might be associated with the seasonal variations of biomass burning in each PSA and transport pathway and processes. Details of BC transport and origins will be discussed in later sections.

In addition to seasonal features of EBC concentrations, AAE showed clear seasonal variation at Syowa (Figs. 3b and 3d). AAE ranged mostly in 0.5–1.0 in April–October and 1.0–1.5 in summer during our measurement at Syowa. AAE increased slightly in the maximum of EBC concentrations (September–October). Earlier works confirmed AAE = 1 in the case of dominance of external mixed EBC (e.g., Bond et al., 2013; references therein). By contrast, AAE of the coated BC (i.e. internal mixed EBC) is lower than 1 (Leck and Cappa, 2010; Bond et al., 2013). Furthermore, the mixing of organic aerosols and minerals can engender high AAE, for instance, 3.5–7 for organics and typically 2–3 for minerals (e.g., Bond et al., 2013, and references therein). EBC is expected to be transported from mid-latitudes and low latitudes, as suggested by Fiebig et al. (2009) and Hara et al. (2010). Therefore, EBC mixing states might be changed by aging processes near source regions and during long-range transport (Shiraiwa et al., 2007; Saleh et al., 2013, 2014; Ueda et al., 2018). Indeed, Ueda et al. (2018) showed that EBC was present mostly as internal mixtures in the marine boundary layer (MBL) of the Southern Ocean. Therefore, lower AAE in April–October suggests that EBC was dominantly present as the coated EBC particles (internal mixtures) at Syowa. Because of the slight increase of AAE, mixing states of EBC might differ somewhat in September–October with the maximum of EBC concentrations. By contrast, high AAE in summer cannot be explained solely by EBC aging processes. Earlier studies have indicated high concentrations of mineral particles (Al) at Neumayer in the summer (Wagenbach, 1996; Weller et al., 2013). Therefore, it is necessary to assess the effects of organic aerosols and mineral particles on optical absorption.

Considering strong optical absorption by organics (i.e. BrC) in UV range, contribution of organics can be assessed from comparison between AAE in UV-IR channels ($AAE_{UV\text{-}IR}$) and AAE in Vis-IR channels ($AAE_{Vis\text{-}IR}$). Figure 4 depicts the relation between $AAE_{UV\text{-}IR}$ and $AAE_{Vis\text{-}IR}$. High correlation of $AAE_{UV\text{-}IR}$ and $AAE_{Vis\text{-}IR}$ was observed throughout the year. Monthly median ratios of $AAE_{Vis\text{-}IR}/AAE_{UV\text{-}IR}$ were 0.55–0.92 (Fig. 4b). Particularly, higher ratios (0.88–0.92) were found in the spring maximum of the EBC concentration (September–November). Because of high optical absorption of organic aerosols in UV channels (e.g., Bond et al., 2013), the difference suggests that organic aerosols, rather than effects of mineral particles, contributed to optical absorption and AAE. Results of linear regression, as portrayed in Fig. 4, indicated that intercepts had negative values in all months. Particularly, larger negative values (≤ 0.4) were obtained for October–November (Fig. 4d). When optical absorption in UV regions was made stronger by organic aerosols (i.e. BrC), the intercepts can have larger negative values. Considering that EBC in EBC maximum might be associated with biomass burning and long-range transport (details are discussed in later sections), it is expected that large amounts of biomass-burning-origin organic aerosols are transported to Antarctica. Indeed, the concentrations of particulate oxalate show a spring maximum (Fig. S1 in Supplementary Materials). Therefore, the larger negative intercepts might result from effects of organic aerosols derived from biomass burning.

Considering that EBC concentrations decreased in summer at Syowa, organic aerosols and their precursors might be supplied not from combustion processes but from the other sources. One major organic aerosol constituent was found to be $CH_3SO_3^-$, which is involved with oceanic bioactivity and photochemical processes in the Antarctic coasts during summer (e.g., Minikin et al., 1998; Preunkert et al., 2008). Indeed, $CH_3SO_3^-$ was identified as an internal mixture with SO_4^{2-} in the Antarctic coasts (Hara et al., 1995). In addition, aerosol particles containing SO_4^{2-} were present as strong acidic droplets in the Antarctic troposphere (e.g., Hara et al., 2013, references therein). Therefore, $CH_3SO_3^-$ might be present as an acidic solution in aerosols in the Antarctic troposphere during summer. CH_3SO_3H aqueous solutions have strong optical absorption in UV (Fig. S2 in Supplementary Materials). Indeed, the imaginary refractive index has a weak band in the UV region (Myhre et al., 2004).

© Author(s) 2019. CC BY 4.0 License.

Therefore, seasonal features of AAE might be associated with EBC aging processes and with the presence and mixing of organic aerosols (e.g. CH_3SO_3H) derived from oceanic bioactivity and mineral particles on the Antarctic coasts.

In contrast to the AAE summer maximum, AAE increased slightly in the spring EBC maximum (Fig. 3). Moreover, slopes in the linear regressions during the EBC maximum exhibited maximum (slopes ≥ 1) at Syowa, as portrayed in Fig. 4. The EBC concentrations and biomass-burning-origin organic aerosols increased in the spring maximum, whereas the EBC concentrations decreased and the concentrations of organic aerosols such as $CH_3SO_3^-$ derived from oceanic bioactivity increased during summer. In addition, the optical absorption of BrC was found to vary greatly depending on the origins of BrC (Moschos et al., 2018). Therefore, these differences might engender seasonal features of aerosol optical absorption properties related to the concentrations of EBC and organic aerosols, optical absorption properties of BrC, and mixing states of aerosol constituents at Syowa.

3.2 Air mass origins at Syowa Station, Antarctica

As described above, EBC concentrations at Syowa were found to show clear seasonal variations. To elucidate the seasonal features, we must compare the seasonal features of EBC concentrations to seasonal variations of transport processes and EBC source strength in the Southern Hemisphere. First, we compare EBC data to the air mass history at Syowa. Figure 5 depicts density maps of end-points of the 5-day backward trajectory (i.e. air mass origins in this study). The transport pathway is classifiable roughly into (1) poleward flow from the Southern Ocean, (2) westward flow along the coastline, and (3) outflow from the Antarctic continent to the coasts. These flow patterns were identified through the year at Syowa. In the poleward flow from the ocean, air masses were transported mostly from the Atlantic Ocean of >40°S and from the Indian Ocean of >50°S within 5 days, although transport from the Atlantic Ocean at ca. 30°S was found in some cases. These flow patterns corresponded to direct EBC transport pathway to the Antarctic coasts suggested by Fiebig et al. (2009) and Hara et al. (2010). In westward flows, the air mass origins for the prior 5 days were distributed to the Antarctic coasts of approx. 150°E. Although some air masses at 150°E were transported even in winter, the density around the coasts at 140–150°E was higher in summer, particularly during November–January. Wintering research stations such as Mawson (67°36′S, 62°52′E), Zhongshang (69°22′S, 76°22′E), and Dumont d'Urville (66°40′S, 140°00′E) have been operated at the coasts of 40–150°E. Although EBC can be emitted from these stations by human activity, Syowa is too distant to have any strong effect on EBC concentrations by local EBC emission in these stations, as suggested by Hagler et al. (2008), because of the slight EBC source strength. Furthermore, outflows from the Antarctic continent were observed throughout the year. The trajectory density on the Antarctic continent was especially lower at high latitudes during summer. By contrast, the air mass origins were distributed extensively in the Antarctic continent during winter. This difference implies that the transport strength of the outflow from the Antarctic continent had remarkable seasonal change. In addition, air masses came occasionally from the Pacific Ocean sector across the Antarctic continent.

To understand the spatial and vertical motion of air masses, Fig. 6 shows vertical density plots of the trajectory. In the cases of the poleward flow from the ocean, air masses passed through the lower troposphere, mainly in the MBL and partly in the lower free troposphere (LFT). By contrast, air masses came mostly from the free troposphere (FT) over the Antarctic continent. In addition to the descent flow, air masses near the surface on the continent were also transported to Syowa during winter. Most of the end-points of the backward trajectories over the continent were distributed up to ca. 4000 m during summer. However, the distribution of the end-points was expanded to ca. 6000 m over the continent during winter. It is noteworthy that the vertical density maps are shown using the height above ground level. Therefore, the air mass history implies that air masses near tropopause over the continent can flow to the boundary layer (BL) at the Antarctic coasts during winter. This seasonal difference indicates that vertical mixing in the outflow from the Antarctic continent was stronger in the winter than in summer.

© Author(s) 2019. CC BY 4.0 License.

At latitudes of around 70°S, high density was identified below 2000–3000 m. Therefore, air masses in the westward flow passed through the lower troposphere during the summer. Consequently, the following transport patterns and air mass origins at Syowa are classifiable in this study: (1) poleward flow from MBL, (2) poleward flow from LFT, (3) westward flow along the coastal line via BL, (4) westward flow along the coastal line from LFT, (5) outflow from the FT over the Antarctic continent, and (6) outflow from BL over the Antarctic continent.

Here, we use the following criteria to divide each air mass origin: marine, <66°S; coastal, 66–75°S; continental, >75°S; BL, <1500 m; FT, >1500 m. In this study, the areas with passage of air mass for the longest times in the 5-day backward trajectory were identified as air mass origins. Figure 7 depicts seasonal features of air mass origins in each month at Syowa during our measurements (2005–2016). The dominant air mass origins were MBL, coastal BL, coastal FT, and continental FT. The most dominant air mass origins were MBL and coastal BL in November–February. In addition to MBL and coastal BL, the contributions of transport from coastal FT and continental FT increased in February/March – October at Syowa, although year-to-year differences were found in the seasonal variations of air mass origins.

3.3 EBC concentrations in respective air mass origins

We compared the EBC concentrations at Syowa with the air mass history (origins) to elucidate EBC transport processes to the Antarctic coasts and EBC spatial distribution in Antarctica. The backward trajectories were computed every hour. The hourly mean EBC concentration for each air mass origin is presented in Fig. 8. The respective EBC concentrations in MBL and marine FT were higher than those in continental FT and BL. The differences of EBC concentrations for each air mass origin might reflect on the latitudinal gradient and spatial distribution of EBC. This latitudinal gradient was found to be consistent with results reported from earlier works (Hansen et al., 1988; Bodhaine, 1995; Wolff and Cachier, 1998; Weller et al., 2013). Although different instruments were used for EBC measurements among Syowa (7 wavelength aethalometer, AE31), Halley (aethalometer: AE10), Neumayer (aethalometer: AE10 and Multi-angle absorption photometer (MAAP)), and South Pole (particulate soot absorption photometer (PSAP)), the EBC measurement principles were similar (i.e. filter-base optical attenuation measurement). Because of the lower (negligible) EBC source strength on the Antarctic continent, the latitudinal distributions might result from dilution during transport from low latitudes and mid-latitudes and dry/wet deposition of EBC onto the snow surface.

Measurements show that EBC concentrations in each air mass origin were higher in September–November. Particularly, EBC concentrations in MBL increased gradually during May–June. Seasonal features in MBL suggest that EBC concentrations have seasonal variations in MBL of the Southern Ocean in Atlantic and Indian Ocean sectors. Although few EBC measurements were made through the year in the Southern Ocean, EBC concentrations in Amsterdam Islands (mid-latitude in Indian Ocean: 37°50′S, 77°30′E) showed strong seasonal variations of EBC concentrations with a maximum in July–September (Wolf and Cachier, 1998; Scaire et al., 2009). Previous ship-borne EBC measurements showed EBC concentrations of <10 ng m^{-3} in January–April over the southern Indian Ocean (<56°S) (Moorthy et al., 2005), and 20–80 ng m^{-3} in October–December over the Indian Ocean–Southern Ocean (34–59°S) (Sakerin et al., 2007). In MBL of the southern Atlantic Ocean (close to South America) to the Southern Ocean, the EBC concentrations were <10–160 ng m^{-3} in October–November and <10–120 ng m^{-3} in February–March (Evangelista et al., 2007). Although we must consider geographical locations of these EBC measurements, these EBC concentrations were several to ten times higher than the background EBC concentrations at the Antarctic coasts, and corresponded to higher EBC concentrations at Syowa in the cases of poleward transport via MBL and MFT. Furthermore, seasonal variations and distributions of CO concentrations in the Southern Hemisphere exhibited the spring maximum corresponding to outflow from the continents and fire counts in each PSA (Gros et al., 1999; Edwards et al., 2006a, 2006b). In addition, Edwards et al. (2006a) reported that high CO concentrations in Africa appeared in earlier months

© Author(s) 2019. CC BY 4.0 License.

than those in other PSAs such as South America. This difference was similar to differences of seasonal features of EBC concentrations at Syowa, as described above. Considering the highest EBC concentrations in MBL, direct transport via MBL contributed significantly to EBC concentrations in the Antarctic coasts. As suggested by Fiebig et al. (2009) and Hara et al. (2010), the transport pathway was involved with cyclone activity in the Southern Ocean. The end-points of the backward trajectory were distributed in the lower troposphere in the marine sector (<66°S), as depicted in Fig. 6. Therefore, direct EBC transport to the Antarctic coasts via the free troposphere might occur at altitudes lower than 3000 m.

In spite of lower EBC concentrations in the continental FT, seasonal features of EBC concentrations were maximum in October–November in the continental FT, in contrast to decreased EBC concentrations in MBL and MFT from November. Additionally, the EBC concentrations in the continental FT were higher than the EBC concentrations measured at the South Pole (Hansen et al., 1988; Wolff and Cachier, 1998). Similar to the latitudinal gradient, the difference in EBC concentrations is expected to be related to the vertical gradient of EBC concentrations over the plateau (inland) area. Indeed, Schwartz et al. (2013) reported higher EBC concentrations in the upper free troposphere than in the lower troposphere over the Antarctic coasts. This fact implies that EBC was supplied to the Antarctic regions also via the upper free troposphere. Indeed, airplane-borne CO_2 measurements over Syowa revealed that CO_2 was transported from mid-latitudes to Antarctica via the upper troposphere (>5 km) (Murayama et al., 1995). Figure 7 shows that no direct flow from the upper free troposphere over marine sector to Syowa was identified. Therefore, EBC in the Antarctic coasts might be supplied also by transport via the upper free troposphere from mid-latitudes, followed by downward flow from the continental FT. Considering the EBC concentrations in the continental FT, EBC transport via the upper FT might make a small contribution on EBC concentrations at Syowa.

3.4 Origins and potential source areas of EBC in the Antarctic coast (Syowa)

Trajectory analysis can provide important information about the relation between EBC concentrations and air mass history, but it cannot let us know the origins and PSA of EBC measured at Syowa (Antarctic coasts). To elucidate the BC origins and PSA, we can compare the EBC data to EBC concentrations simulated using the CHASER model. Figure 9 presents seasonal features of monthly median EBC concentrations measured at Syowa and the model-BC concentrations. Model-BC concentrations tended to be lower than the EBC concentrations in the summer, although the model-BC concentrations were higher during the spring maximum. This difference might result from positive bias by filter-based BC measurement techniques such as the use of aethalometer (e.g., Bond et al., 2013) and uncertainty of EBC transport strength to the Antarctic regions involved with aging and deposition processes in the model simulation. However, the range of EBC concentrations measured at Syowa matched those at the other coastal stations (Neumayer and Halley) (Wolff and Cachier, 1998; Weller et al., 2013). Furthermore, the range of the model-BC concentrations and their seasonal features were consistent with those of the observed data (median EBC concentrations): $[\text{model-BC}] = 0.935 \times [\text{EBC}]_{\text{observed}} - 0.0588$ (R=0.5771). Therefore, we attempted to discuss EBC origins and PSA using the model data presented below.

In this study, the following EBC origins were classified: (1) biomass burning (BB) such as forest and savanna fires, (2) fossil fuel combustion (FFC), and (3) other combustion (OC). Because "other combustion" includes combustion of biomaterials (e.g. wood fuels), most of the other combustion data were those of biomass burning in a broad sense. Contributions of potential EBC origins showed clear seasonal features as presented in Fig. 10a. Biomass burning was dominant (50–80%, mean 70.7%) in spring EBC maximum at Syowa. By contrast, the FFC contribution was lower (10–20%, mean 14.8%) than the BB contribution. As described above, earlier studies have indicated that EBC in the Antarctic troposphere was supplied by BB in the Southern Hemisphere and long-range transport (Wolff and Cachier, 1998; Fiebig et al., 2009; Hara et al., 2010; Weller et al., 2013). Although the OC contribution increased to more than 50% in autumn–winter (February–June), the periods corresponded to the lower EBC concentrations at Syowa.

© Author(s) 2019. CC BY 4.0 License.

Figure 10b shows that the BB-model-BC concentrations reached their maximum values at Syowa during August–October, although high BB-model-BC concentrations were found occasionally in July and November. South America, southern Africa, and Australia were identified as the important PSAs of BC at Syowa (Fig. S3 in Supplementary Materials). Particularly, BB from South America and southern Africa contributed more than 90% of BB-model-BC in the spring maximum (Fig. S3). The contributions of BB in South America and southern Africa were of a similar range, although a slight year-to-year difference was found in their contributions. Moreover, BB-model-BC concentrations in southern Africa increased often in earlier months than they did in South America. The BB-model-BC concentrations in Australia increased in November (after the spring maximum) at Syowa. Contributions and concentrations of BB-model-BC in Australia increased drastically after the spring maximum (October–November). However, BB-model-BC concentrations in Australia were considerably lower at Syowa than those in southern Africa and South America. These differences of seasonal features of BB-model-BC concentrations/contribution at Syowa in each PSA might be associated with (1) the seasonality of occurrence of BB in each PSA and (2) transport strength from each PSA to Syowa. Indeed, earlier works showed similar seasonal features of fire counts, burned areas, and CO concentrations/emission in/over South America, southern Africa, and Australia (Edwards et al., 2006a, 2006b; van der Werf et al., 2006; Giglio et al., 2013). Furthermore, seasonal features of fire counts and aerosol absorption optical depth measured by satellite (OMI) showed a one-month lag in the maximum of aerosol absorption optical depth (September for Africa and October for South America; Torres et al., 2010). In addition, mineral dust and atmospheric substances from biomass burning can outflow eastwardly from the continents (Edwards et al., 2006a; Fiebig et al., 2009; Hara et al., 2010; Neff and Bertler, 2015). The eastward flow patterns in the Southern Hemisphere are presented in Fig. 5, suggesting strongly that BB-model-BC from southern Africa and South America can be transported directly to Syowa, but rarely from Australia. Consequently, BB-model-BC from Australia might have usually a lower contribution at Syowa. Model simulation showed high BB-model-BC concentrations in Australia in later spring of 2011 and 2012. Higher EBC concentrations were observed in November 2011 than in November in other years. What was the transport process of BB-model-BC from Australia to Syowa? As shown by Neff and Bertler (2015), air masses extended from Australia to the Antarctic coasts in the Pacific Ocean sector. For that reason, BB-model-BC originated in Australia can be transported to Syowa, considering the westward flow along with the coastal line as described above. Similarly, BB-model-BC in southern Africa might contribute only slightly to EBC observed at Halley and Neumayer because of rarely directed transport. Therefore, lag in the spring maximum of EBC concentrations among Syowa, Halley and Neumayer might be attributed to the seasonality of BB phenomena in each PSA and transport strength from PSA to each station.

The BB-model-BC concentrations at Syowa started increasing in June. They increased considerably in August. The EBC concentrations increased gradually after May–June. In contrast to BB-model-BC, the concentrations of FFC-model-BC and OC-model-BC started increasing in May–June. Furthermore, good correlation was obtained between the concentrations of FFC-model-BC and OC-model-BC (R^2=0.9675), with lower correlation in BB-model-BC–FFC-model-BC (R^2 = 0.4175) and BB-model-BC–OC-model-BC (R^2 = 0.3654). Year-to-year variation of FFC-model-BC was much less than that of BB-model-BC. Therefore, seasonal features of FFC-model-BC and OC-model-BC might reflect variations of transport strength from each PSA to Syowa. South America was found to be the most-contributing PSA (34.1–82.4%; mean, 63.6%) in FFC-model-BC at Syowa through the year (Fig. 10c). The FFC-model-BC contribution in southern Africa was 7.4–54.0% (mean, 20.9%). In spite of the larger BB contribution in Australia, FFC had a contribution of only 3.9–17.5% (mean, 8.0%), which was lower than that of BB-model-BC in Australia. The contributions of FFC and OC differed greatly from those of BB, especially in South America and southern Africa. Considering that both BB-model-BC and FFC-model-BC outflowed simultaneously from each PSA, the transport processes cannot account for the difference of contribution between BB-model-BC and FFC-model-BC. Unlike FFC, BB has strong seasonality in each PSA as described above. Furthermore, fossil fuel consumption depends on

© Author(s) 2019. CC BY 4.0 License.

the gross domestic product (GDP). Indeed, the aggregated GDPs of countries in South America are the largest in the Southern Hemisphere. Therefore, the difference of FFC-model-BC contribution might reflect the fossil fuel consumption related to population and economic activity in the respective PSAs. Because of rapid population expansion in countries of southern Africa recently, it is expected that more EBC can be released by fossil fuel combustion in southern Africa in the future. Therefore, continual EBC measurements at the Antarctic coasts must monitor the atmospheric substances (e.g. EBC) originating from combustion processes in the Southern Hemisphere.

The concentrations of BB-model-BC, FFC-model-BC, and OC-model-BC showed minima during February–April/May, although poleward flow via MBL and MFT occurred as portrayed in Fig. 7. The following likelihoods were regarded as contributing factors: seasonal features of (1) EBC source strength and (2) air mass history (i.e. air mass origins). As demonstrated by earlier work (Edwards et al., 2006a, 2006b; van den Werf et al., 2006; Torres et al., 2010), BB in South America, southern Africa, and Australia showed strong seasonal variation, with lower fire counts in February–April/May because of large precipitation amounts. Results show that BB was the greatest factor affecting EBC concentrations in the Southern Hemisphere. Therefore, the seasonal features of biomass burning might have an effect on EBC concentrations in the Antarctic regions. However, it is noteworthy that FFC-model-BC concentrations also showed a minimum in February–April/May at Syowa. This fact cannot be explained by the seasonal features of BB. Assuming that FFC-model-BC is useful as proxy for transport from the continents with human activity to the Antarctic regions, the EBC minimum in February–April/May might be associated not only with the features of BB, but also with the features of the air mass history. As portrayed in Fig. 7, the contributions of air masses identified as coastal BL and continental FT increased in February–April/May in the most years, and particularly in 2010. A similar tendency (high contribution of the upper atmosphere at surface of Antarctic coasts in austral autumn) was also identified from FLEXPART analysis by Stohl and Sodemann (2010). The EBC source strength in the Antarctic region, especially in FT over the Antarctic continent, is less or negligible. Therefore the seasonal features of BB in the Southern Hemisphere and air mass origins at Syowa might engender the EBC minimum at Syowa.

4. Conclusion

EBC measurements were conducted at Syowa Station, Antarctica from February 2005. Long-term trends over approximately a decade were almost constant. Seasonal features of EBC concentrations at Syowa showed maximum values in September–October and minimum values in February–April, similar to the seasonal features observed at Neumayer, Halley, and the South Pole (Wolff and Cachier, 1998; Weller et al., 2013). AAE exhibited clear seasonal features with high (1.0–1.5) in summer and low (0.5–1.0) in winter at Syowa. The AAE seasonal features imply that EBC is present as internal mixtures in winter–spring. High AAE in the summer might result from optical absorption mainly by organic aerosols (such as methansulfonic acid) derived from oceanic bioactivity. Comparison to results of backward trajectory analysis showed that direct poleward flow via MBL and lower free troposphere engender high EBC concentrations at Syowa. Additionally, EBC was burdened from mid-latitudes through the upper troposphere and then transported from the continental free troposphere to Syowa. Comparison between the observation and model simulation indicated that biomass burning in South America and southern Africa had the greatest effect on model-BC at Syowa. The contributions of South America and southern Africa were of a similar range. In addition, South America is the most important PSA of model-BC derived from fossil fuel combustion. Furthermore, seasonal features of air mass origins (high contribution of continental free troposphere and coastal boundary layer) might be attributable to EBC minimum in February–April at Syowa, in addition to the seasonal variation of EBC source strength in each PSA. With population growth and economic development in the Southern Hemisphere, more anthropogenic BC might be released in the future. Moreover, the PSA of EBC is apparently different between Neumayer in the Atlantic Ocean sector and Syowa in the Indian Ocean sector. Therefore, continual EBC measurements must be taken at Syowa Station to elucidate the EBC burden into the Antarctic regions and effects on surface albedo and atmospheric aerosol absorbing in the future. Furthermore, these

© Author(s) 2019. CC BY 4.0 License.

data can provide us better understanding and interpretation on EBC records in the Antarctic ice cores from the viewpoints of transport processes and biomass burning history.

Appendix

List of acronym in this study

AAE Absorption Ångström exponent
AAE_{UV-IR} Absorption Ångström exponent in range of UV-IR
AAE_{Vis-IR} Absorption Ångström exponent in range of Vis-IR
BB Biomass burning
BC Black carbon
BL Boundary layer
BrC Brown carbon
C_{abs} Optical absorption cross-section
EBC Equivalent black carbon. In this study, we use the term EBC for the corrected mass BC concentrations and the measured BC concentrations using filter-base optical techniques in previous works.
EC Elemental carbon
ENSO El Niño-Southern Oscillation
FFC Fossil fuel combustion
FT Free troposphere
GDP The gross domestic product
IR Infrared
JARE Japanese Antarctic research expedition
LFT Lower free troposphere
MAAP Multi-angle absorption photometer
MBL Marine boundary layer
Model-BC BC concentrations obtained by model simulation
NMVOCs Non-methane volatile organic carbons
OC Other combustion
PSA Potential source area
PSAP Particulate soot absorption photometer
UV Ultraviolet
Vis Visible

Author contribution

K.H., K.O., MS and T.Y. designed the experiments, which were conducted by K.O., K.H., and M.Y. K.H. wrote the manuscript and analyzed BC data and backward trajectory. KH and MY analyzed and discussed aerosol optical properties. KS and TO developed and conducted the tagged BC simulation using CAHSER model. All authors reviewed and commented on the paper.

© Author(s) 2019. CC BY 4.0 License.

Acknowledgements

We would like to thank Y. Aoyama, Y. Takeda, T. Masunaga, T. Kinase, C. Ikeda, Y. Hayakawa, J. Matsushita, and I. Arakawa for help with aerosol measurements at Syowa Station, Antarctica, and C. Nishita-Hara for measurement of absorbance of MSA aqueous solution. We obtained MACC reanalysis data from the European Centre for Medium-Range Weather Forecasts (ECMWF). This study was supported by the "Observation project of global atmospheric change in the Antarctica" for JARE 43–47, and Grants-in-Aid for Scientific Research (B) (no. 22310013 and 15H02806, PI: K. Hara) from the Ministry of Education, Culture, Sports, Science and Technology of Japan.

References

Aarons, S. M., Aciego, S. M., Gabrielli, P., Delmonte, B., Koornneef, J. M., Wegner, A., and Blakowski, M. A.: The impact of glacier retreat from the Ross Sea on local climate: Characterization of mineral dust in the Taylor Dome ice core, East Antarctica, Earth and Planetary Science Letters, 444, 34–44, doi:10.1016/j.epsl.2016.03.035, 2016.

Albani, S., Mahowald, N., Delmonte, B., Maggi, V., and Winckler, G.: Comparing modeled and observed changes in mineral dust transport and deposition to Antarctica between the Last Glacial Maximum and current climates, Climate Dynamics, 38(9-10), 1731–1755, doi:10.1007/s00382-011-1139-5, 2012.

Aoki, T., Kuchiki, K., Niwano, M., Kodama, Y., Hosaka, M., and Tanaka, T.: Physically based snow albedo model for calculating broadband albedos and the solar heating profile in snowpack for general circulation models, Journal of Geophysical Research, 116(D11), doi:10.1029/2010JD015507, 2011.

Arienzo, M., McConnell, J., Murphy, L., Chellman, N., Das, S., Kipfstuhl, S., and Mulvaney, R.: Holocene black carbon in Antarctica paralleled Southern Hemisphere climate, Journal of Geophysical Research: Atmospheres, (13), doi:10.1002/2017JD026599, 2017.

Bisiaux, M. M., Edwards, R., McConnell, J. R., Curran, M. A. J., Van Ommen, T. D., Smith, A. M., Neumann, T. A., Pasteris, D. R., Penner, J. E., and Taylor, K.: Changes in black carbon deposition to Antarctica from two high-resolution ice core records, 1850–2000 AD, Atmos. Chem. Phys., 12, 4107–4115, https://doi.org/10.5194/acp-12-4107-2012, 2012.

Bodhaine, B. A.: Aerosol absorption measurements at Barrow, Mauna Loa and the South Pole, Journal of Geophysical Research: Atmospheres (1984–2012), 100(D5), 8967–8975, doi:10.1029/95JD00513, 1995.

Bond, T. C, Doherty, S. J., Fahey, D. W., Forster, P. M., Berntsen, T., DeAngelo, B. J., Flanner, M. G., Ghan, S., Kärcher, B., Koch, D., Kinne, S., Kondo, Y., Quinn, P. K., Sarofim, M. C., Schultz, M. G., Schulz, M., Venkataraman, C., Zhang, H., Zhang, S., Bellouin, N., Guttikunda, S. K., Hopke, R. K., Jacobson, M. Z., Kaiser, J. W., Klimont, Z., Lohmann, U., Schwarz, J. P., Shindell, D., Storelvmo, T., Warren, S. G., and Zender, C. S.: Bounding the role of black carbon in the climate system: A scientific assessment, Journal of Geophysical Research: Atmospheres, 118, doi:10.1002/jgrd.50171, 2013.

Bory, A., Wolff, E., Mulvaney, R., Jagoutz, E., Wegner, A., Ruth, U., and Elderfield, H.: Multiple sources supply eolian mineral dust to the Atlantic sector of coastal Antarctica: Evidence from recent snow layers at the top of Berkner Island ice sheet, Earth and Planetary Science Letters, 291(1-4), 138–148, doi:10.1016/j.epsl.2010.01.006, 2010.

Chang, C., Han, C., Han, Y., Hur, S., Lee, S., Motoyama, H., Hou, S., and Hong, S.: Persistent Pb pollution in central East Antarctic snow: a retrospective assessment of sources and control policy implications, Environmental Science & Technology, doi:10.1021/acs.est.6b03209, 2016.

Chaubey, J., Moorthy, B., Nair, V., and Tiwari, A.: Black carbon aerosols over coastal Antarctica and its scavenging by snow during the Southern Hemispheric summer, Journal of Geophysical Research, doi:10.1029/2009JD013381, 2010.

Collaud-Coen, M., Weingartner, E., Apituley, A., Ceburnis, D., Fierz-Schmidhauser, R., Flentje, H., Henzing, J. S., Jennings, S. G., Moerman, M., Petzold, A., Schmid O., and Baltensperger, U.: Minimizing light absorption measurement artifacts of

© Author(s) 2019. CC BY 4.0 License.

the Aethalometer: evaluation of five correction algorithms, Atmospheric Measurement Techniques, doi:10.5194/amt-3-457-2010, 2010.

Deckker, P., Norman, M., Goodwin, I., Wain, A., and Gingele, F.: Lead isotopic evidence for an Australian source of aeolian dust to Antarctica at times over the last 170,000 years, Palaeogeography, Palaeoclimatology, Palaeoecology, 285(3-4), 205–223, doi:10.1016/j.palaeo.2009.11.013, 2010.

Delmonte, B., Andersson, P. S., Hansson, M., Schöberg, H., Petit, J. R., Basile-Doelsch, I., and Maggi, V.: Aeolian dust in East Antarctica (EPICA-Dome C and Vostok): Provenance during glacial ages over the last 800 kyr, Geophysical Research Letters, doi:10.1029/2008GL033382, 2008.

Delmonte, B., Petit, J. R., Andersen, P. S., Basile-Doelsch, I., Maggi, V., and Lipenkov, V.: Dust size evidence for opposite regional atmospheric circulation changes over east Antarctica during the last climatic transition, Climate Dynamics, doi:10.1007/s00382-004-0450-9, 2004.

Edwards, D. P., Emmons, L. K., Gille, J. C., Chu, A., Attié, J.-L., Giglio, L., Wood, S. W., Haywood, J., Deeter, M. N., Massie, S. T., Ziskin, D. C., and Drummond, J. R.: Satellite-observed pollution from Southern Hemisphere biomass burning, Journal of Geophysical Research, 111, D14312, doi:10.1029/2005JD006655, 2006a.

Edwards, D. P., Pétron, G., Novelli, P., Emmons, L., Gille, J. C., and Drummond, J. R.: Southern Hemisphere carbon monoxide interannual variability observed by Terra/Measurement of Pollution in the Troposphere (MOPITT), Journal of Geophysical Research, 111, D16303, doi:10.1029/2006JD007079, 2006b.

Evangelista, H., Maldonado, J., Godoi, R. H. M.,, Pereira, E. B., Koch, D., Tanizaki-Fonseca, K., Grieken, V., R., Sampaio, M., Setzer, A., Alencar, A., and Gonçalves, S. C.: Sources and transport of urban and biomass burning aerosol black carbon at the South-West Atlantic Coast, Journal of Atmospheric Chemistry, 56(3), 225–238, doi:10.1007/s10874-006-9052-8, 2007.

Fiebig, M., Lunder C. R., and Stohl, A.: Tracing biomass burning aerosol from South America to Troll Research Station, Antarctica, Geophysical Research Letters, doi:10.1029/2009GL038531, 2009.

Flanner, M., Zender, C., Randerson, J., and Rasch, P.: Present-day climate forcing and response from black carbon in snow, Journal of Geophysical Research, 112(D11), doi:10.1029/2006JD008003, 2007.

Gabrielli, P., Wegner, A., Petit, J., Delmonte, B., Deckker, P., Gaspari, V., Fischer, H., Ruth, U., Kriews, M., Boutron, C., Cescon, P., and Barbante, C.: A major glacial-interglacial change in aeolian dust composition inferred from Rare Earth Elements in Antarctic ice, Quaternary Science Reviews, doi:10.1016/j.quascirev.2009.09.002, 2010.

Gambaro, A., Zangrando, R., Gabrielli, P., Barbante, C., and Cescon, P.: Direct determination of levoglucosan at the picogram per milliliter level in Antarctic ice by high-performance liquid chromatography/electrospray ionization triple quadrupole mass spectrometry, Anal. Chem., 80(5), 1649–1655, doi:10.1021/ac701655x, 2008.

Gassó, S., Stein, A., Marino, F., Castellano, E., Udisti, R., and Ceratto, J.: A combined observational and modelling approach to study modern dust transport from the Patagonia desert to East Antarctica, Atmospheric Chemistry and Physics, 10(17), 82878303, doi:10.5194/acp-10-8287-2010, 2010.

Gelencsér, A: Chapter 3: Major carbonaceous particle types and their sources in “Carbonaceous aerosol”, pp.45-147, Springer, 2004.

Giglio, L., Randerson, J., and Werf, G.: Analysis of daily, monthly, and annual burned area using the fourth-generation global fire emissions database (GFED4), Journal of Geophysical Research: Biogeosciences, 118(1), 317–328, doi:10.1002/jgrg.20042, 2013.

Gili, S., Gaiero, D., Goldstein, S., Chemale, F., Koester, E., Jweda, J., Vallelonga, P., and Kaplan, M.: Provenance of dust to Antarctica: A lead isotopic perspective, Geophysical Research Letters, 43, doi:10.1002/2016GL068244, 2016.

© Author(s) 2019. CC BY 4.0 License.

Graf, H.-F., Shirsat, S. V., Oppenheimer, C., Jarvis, M. J., Podzun, R., and Jacob, D.: Continental scale Antarctic deposition of sulphur and black carbon from anthropogenic and volcanic sources, Atmospheric Chemistry and Physics, doi:10.5194/acp-10-2457-2010, 2010.

Hadley, O. and Kirchstetter, T.: Black-carbon reduction of snow albedo, Nat. Clim. Change, 2(6), 437–440, doi:10.1038/nclimate1433, 2012.

Hagler, G., Bergin, M., Smith, E., Town, M., and Dibb, J.: Local anthropogenic impact on particulate elemental carbon concentrations at Summit, Greenland, Atmospheric Chemistry and Physics, doi:10.5194/acp-8-2485-2008, 2008.

Hansen, A. D. A., Bodhaine, B. A., Dutton, E. G., Schnell, R. C.: Aerosol black carbon measurements at the South Pole: Initial results, 1986–1987, Geophys. Res. Lett., 15, 1193-1196 (doi:10.1029/GL015i011p01193), 1988.

Hansen, A., Lowenthal, D., Chow, J., and Watson, J.: Black carbon aerosol at McMurdo station, Antarctica, Journal of the Air & Waste Management Association, 51(4), 593–600, doi:10.1080/10473289.2001.10464283, 2001.

Hara, K., Kikuchi, T., Furuya, K., Hayashi, M., and Fujii, Y.: Characterization of Antarctic aerosol particles using laser microprobe mass spectrometry, Environmental Science & Technology, 30, 385-391, doi:10.1021/es9407305, 1996.

Hara, K., Osada, K., Yabuki, M., Hashida, G., Yamanouchi, T., Hayashi, M., Shiobara, M., Nishita, C., and Wada, M.: Haze episodes at Syowa Station, coastal Antarctica: Where did they come from?, Journal of Geophysical Research, 115(D14), doi:10.1029/2009JD012582, 2010.

Hara, K., Osada, K., and Yamanouchi, T.: Tethered balloon-borne aerosol measurements: seasonal and vertical variations of aerosol constituents over Syowa Station, Antarctica, Atmospheric Chemistry and Physics, 13(17), 91199139, doi:10.5194/acp-13-9119-2013, 2013.

Hu, Q.-H., Xie, Z.-Q., Wang, X.-M., Kang, H., and Zhang, P.: Levoglucosan indicates high levels of biomass burning aerosols over oceans from the Arctic to Antarctic, Scientific Reports, 3, 3119, doi:10.1038/srep03119, 2013.

Ito, A., Ito, A., and Akimoto, H.: Seasonal and interannual variations in CO and BC emissions from open biomass burning in Southern Africa during 1998–2005, Global Biogeochemical Cycles, doi:10.1029/2006GB002848, 2007.

Krinner, G., Petit, J.-R., and Delmonte: Altitude of atmospheric tracer transport towards Antarctica in present and glacial climate, Quaternary Science Reviews, doi:10.1016/j.quascirev.2009.06.020, 2010.

Li, F., Ginoux, P., and Ramaswamy, V.: Transport of Patagonian dust to Antarctica, Journal of Geophysical Research: Atmospheres (1984–2012), 115(D18), doi:10.1029/2009JD012356, 2010.

Minikin, A., Legrand, M., Hall, J., Wagenbach, D., Kleefeld, C., Wolff, E., Pasteur, E., and Ducroz, F.: Sulfur-containing species (sulfate and methanesulfonate) in coastal Antarctic aerosol and precipitation, Journal of Geophysical Research, doi:10.1029/98JD00249, 1998.

Moschos, V., Kumar, N., Daellenbach, K., Baltensperger, U., Prevot, A., and Haddad, I.: Source Apportionment of Brown Carbon Absorption by Coupling UV/Vis Spectroscopy with Aerosol Mass Spectrometry, Environ. Sci. Tech. Let., 5, 302–308, doi:10.1021/acs.estlett.8b00118, 2018.

Moteki, N., Adachi, K., Ohata, S., Yoshida, A., Harigaya, T., Koike, M., and Kondo, Y.: Anthropogenic iron oxide aerosols enhance atmospheric heating, Nat. Commun., 8, 15329, doi:10.1038/ncomms15329, 2017.

Murayama, S., Nakazawa, T., Yamazaki, K, Aoki, S., Makino, Y., Shiobara, M., Fukabori, M., Yamanouchi, T., Shimizu, A., Hayashi, M., Kawaguchi, S., and Tanaka, M.: Concentration variations of atmospheric CO_2 over Syowa Station, Antarctica and their interpretation, Tellus B, 47(4), 375–390, doi:10.1034/j.1600-0889.47.issue4.1.x, 1995.

Myhre, C. E., D'Anna, B., Nicolaisen, F. M., and Nielsen, C. J.: Properties of aqueous methanesulfonic acid: complex index of refraction and surface tension, Appl. Opt., 43(12), 2500–2509, 2004.

Neff, P. and Bertler, N.: Trajectory modeling of modern dust transport to the Southern Ocean and Antarctica, Journal of Geophysical Research: Atmospheres, 120(18), 9303–9322, doi:10.1002/2015JD023304, 2015.

© Author(s) 2019. CC BY 4.0 License.

Novakov, T.: The role of soot and primary oxidants in atmospheric chemistry, Science of the Total Environment, 36, 1–10, doi:10.1016/0048-9697(84)90241-9, 1984.

Pasteris, D., McConnell, J., Das, S., Criscitiello, A., Evans, M., Maselli, O., Sigl, M., and Layman, L.: Seasonally resolved ice core records from West Antarctica indicate a sea ice source of sea salt aerosol and a biomass burning source of ammonium, Journal of Geophysical Research: Atmospheres, n/an/a, doi:10.1002/2013JD020720, 2014.

Pereira, E., Evangelista, H., Pereira, K., Cavalcanti, I., and Setzer, A.: Apportionment of black carbon in the South Shetland Islands, Antarctic Peninsula, Journal of Geophysical Research: Atmospheres (1984–2012), 111(D3), doi:10.1029/2005JD006086, 2006.

Pereira, K., Evanhelista, H., Pereira, E., Simões, J., Johnson, E., and Melo, L.: Transport of crustal microparticles from Chilean Patagonia to the Antarctic Peninsula by SEM-EDS analysis, Tellus B, 56(3), 262–275, doi:10.1111/j.1600-0889.2004.00105.x, 2004.

Planchon, F., Boutron, C., Barbante, C., Cozzi, G., Gaspari, V., Wolff, E., Ferrari, C., and Cescon, P.: Changes in heavy metals in Antarctic snow from Coats Land since the mid-19th to the late 20th century, Earth and Planetary Science Letters, 200(1-2), 207222, doi:10.1016/S0012-821X(02)00612-X, 2002.

Preunkert, S., Jourdain, B., Legrand, M., Udisti, R., Becagli, S., and Cerri, O.: Seasonality of sulfur species (dimethyl sulfide, sulfate, and methanesulfonate) in Antarctica: Inland versus coastal regions, Journal of Geophysical Research, 113(D15), doi:10.1029/2008JD009937, 2008.

Sakerin, S. M.,Smirnov, A., Kabanov, D. M., Pol'kin, V. V., Panchenko, M. V., Holben, B. N., and Kopelevich, O. V.: Aerosol optical and microphysical properties over the Atlantic Ocean during the 19th Cruise of the Research Vessel Akademik Sergey Vavilov, Journal of Geophysical Research, doi:10.1029/2006JD007947, 2007.

Saleh, R., Hennigan, C. J., McMeeking, G. R., Chuang, W. K., Robinson, E. S., Coe, H., Donahue, N. M., and Robinson, A. L.: Absorptivity of brown carbon in fresh and photo-chemically aged biomass-burning emissions, Atmospheric Chemistry and Physics, 13, doi:10.5194/acp-13-7683-2013, 2013.

Saleh, R., Robinson, E., Tkacik, D., Ahern, A., Liu, S., Aiken, A., Sullivan, R., Presto, A., Dubey, M., Yokelson, R., Donahue, N., and Robinson, A.: Brownness of organics in aerosols from biomass burning linked to their black carbon content, Nature Geoscience, 7(9), 647–650, doi:10.1038/ngeo2220, 2014.

Shiraiwa, M., Kondo, Y., Moteki, N., Takegawa, N., Miyazaki, Y., and Blake, D. R.: Evolution of mixing state of black carbon in polluted air from Tokyo, Geophysical Research Letters, doi:10.1029/2007GL029819, 2007.

Shirsat, S. V. and Graf, H. F.: An emission inventory of sulfur from anthropogenic sources in Antarctica, Atmospheric Chemistry and Physics, 9(10), 3397–3408, 2009.

Smith, J., Vance, D., Kemp, R., Archer, C., Toms, P., King, M., and Zárate, M.: Isotopic constraints on the source of Argentinian loess – with implications for atmospheric circulation and the provenance of Antarctic dust during recent glacial maxima, Earth and Planetary Science Letters, doi:10.1016/S0012-821X(03)00260-7, 2003.

Stein, A. F., Draxler, R. R, Rolph, G. D., Stunder, B. J. B., Cohen, M. D., and Ngan, F.: NOAA's HYSPLIT atmospheric transport and dispersion modeling system, Bull. Amer. Meteor. Soc., 96, 2059-2077, doi: 10.1175/BAMS-D-14-00110.1, 2015.

Stohl, A. and Sodemann, H.: Characteristics of atmospheric transport into the Antarctic troposphere, Journal of Geophysical Research, 115(D2), doi:10.1029/2009JD012536, 2010.

Sudo, K., and Akimoto, H.: Global source attribution of tropospheric ozone: Long-range transport from various source regions, J. Geophys. Res., 112, D12302, doi: 10.1029/2006 JD007992, 2007.

Sudo, K., Takahashi, M., Kurokawa, J., and Akimoto, H.: Chaser: A global chemical model of the troposphere, 1. Model description, J. Geophys. Res., 107(D17), 4339, doi: 10.1029/2001JD001113, 2002.

© Author(s) 2019. CC BY 4.0 License.

Takemura, T., Nozawa, T., Emori, S., Nakajima, T. Y., and Nakajima, T.: Simulation of climate response to aerosol direct and indirect effects with aerosol transport-radiation model. Journal of Geophysical Research, 110, D02202, doi:10.1029/2004JD005029, 2005.

Ueda, S., Osada, K., Hara, K., Yabuki, M., Hashihama, F., and Kanda, J. Morphological features and mixing states of soot-containing particles in the marine boundary layer over the Indian and Southern Oceans, Atmos. Chem. Phys., 18, 9207–9224, 2018.

Torres, O., Chen, Z., Jethva, H., Ahn, C., Freitas, S. R., and Bhartia, P. K.: OMI and MODIS observations of the anomalous 2008–2009 Southern Hemisphere biomass burning seasons, Atmos. Chem. Phys., 10, 3505–3513, https://doi.org/10.5194/acp-10-3505-2010, 2010.

Vallelonga, P., Velde, K., Candelone, J.-P., Morgan, V. Boutron, C., and Rosman, K.: The lead pollution history of Law Dome, Antarctica, from isotopic measurements of ice cores: 1500 AD to 1989 AD, Earth and Planetary Science Letters, doi:10.1016/S0012-821X(02)00983-4, 2002.

Vallelonga, P., Gabrielli, P., Balliana, E., Wegner, A., Delmonte, B., Turetta, C., Burton, G., Vanhaecke, F., Rosman, K. J. R., Hong, S., Boutron, C. F., Cescon P., and Barbante, C.: Lead isotopic compositions in the EPICA Dome C ice core and Southern Hemisphere Potential Source Areas, Quaternary Science Reviews, doi:10.1016/j.quascirev.2009.06.019, 2010.

van der Werf, G. R., Randerson, J. T., Giglio, L., Collatz, G. J., Kasibhatla, P. S., and Arellano Jr., A. F.: Interannual variability in global biomass burning emissions from 1997 to 2004, Atmos. Chem. Phys., 6, 3423–3441, 2006.

Wagenbach, D.: Coastal Antarctica: atmospheric chemical composition and atmospheric transport. In: Chemical Exchange Between the Atmosphere and Polar Snow, NATO ASI Series Volume 43 (eds E. W. Wolff and R.C. Bales), Springer-Verlag, Berlin Heidelberg, 173–199, 1996.

Warren, S. G. and Clarke, A. D.: Soot in the atmosphere and snow surface of Antarctica, J. Geophys. Res., 95, 1811–1816, 1990.

Watanabe, S., Hajima, T., Sudo, K., Nagashima, T., Takemura, T., Okajima, H., Nozawa, T., Kawase, H., Abe, M., Yokohata, T., Ise, T., Sato, H., Kato, E., Takata, K., Emori, S., and Kawamiya, M.: MIROC-ESM 2010: model description and basic results of CMIP5-20c3m experiments, Geosci. Model Dev., 4, 845–872, https://doi.org/10.5194/gmd-4-845-2011, 2011.

Wegner, A., Gabrielli, P., Wilhelms-Dick, D., Ruth, U., Kriews, M., De Deckker, P., Barbante, C., Cozzi, G., Delmonte, B., and Fischer, H.: Change in dust variability in the Atlantic sector of Antarctica at the end of the last deglaciation, Climate of the Past, 8(1), 135–147, doi:10.5194/cp-8-135-2012, 2012.

Weingartner, E., Saathoff, H., Schnaiter, M., Streit, N., Bitnar, B., and Baltensperger, U.: Absorption of light by soot particles: determination of the absorption coefficient by means of aethalometers, Journal of Aerosol Science, 34, 1445–1463, doi:10.1016/S0021-8502(03)00359-8, 2003.

Weller, R., Wagenbach, D., Legrand, M., Elsnsser, C., Tian-Kunze, X., and Kónig-Langlo, G.: Continuous 25-yr aerosol records at coastal Antarctica – I: interannual variability of ionic compounds and links to climate indices, Tellus, 63B, 901–919, doi:10.1111/j.1600-0889.2011.00542.x, 2011.

Weller, R., Minikin, A., Petzold, A., Wagenbach, D., and König-Langlo, G.: Characterization of long-term and seasonal variations of black carbon (BC) concentrations at Neumayer, Antarctica, Atmospheric Chemistry and Physics, doi:10.5194/acp-13-1579-2013, 2013.

Wolff, E. and Cachier, H.: Concentrations and seasonal cycle of black carbon in aerosol at a coastal Antarctic station, Journal of Geophysical Research, 103, 11033–11041, doi:10.1029/97JD01363, 1998.

Zangrando, R., Barbaro, E., Vecchiato, M., Kehrwald, N., Barbante, C., and Gambaro, A.: Levoglucosan and phenols in Antarctic marine, coastal and plateau aerosols, Science of the Total Environment, 544, 606–616, doi:10.1016/j.scitotenv.2015.11.166, 2016.

Atmos. Chem. Phys. Discuss., https://doi.org/10.5194/acp-2018-1190
Manuscript under review for journal Atmos. Chem. Phys.
Discussion started: 7 January 2019
© Author(s) 2019. CC BY 4.0 License.

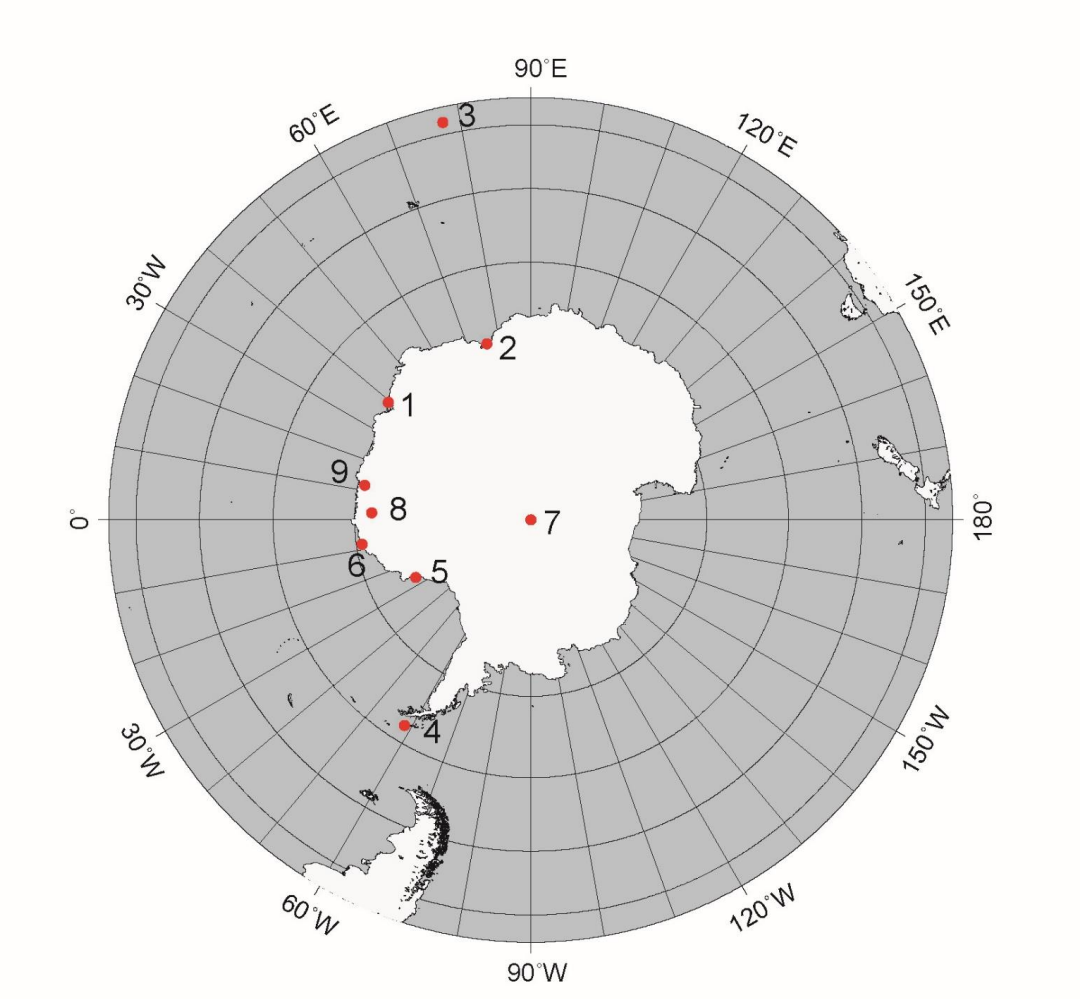

Figure 1: Locations of Syowa Station, and other research stations with BC measurements in Antarctica and the Southern Ocean: 1, Syowa; 2, Larsmann Hills; 3, Amsterdam Island; 4, Ferraz; 5, Halley; 6, Neumayer; 7, South Pole; 8 Troll; and 9, Maitri.

Atmos. Chem. Phys. Discuss., https://doi.org/10.5194/acp-2018-1190
Manuscript under review for journal Atmos. Chem. Phys.
Discussion started: 7 January 2019
© Author(s) 2019. CC BY 4.0 License.

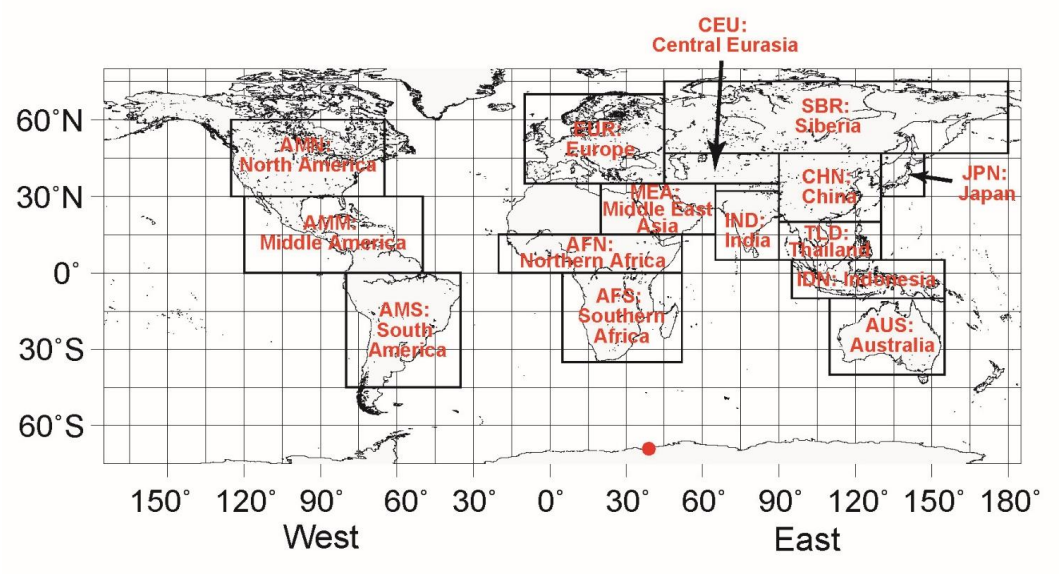

Figure 2: Regional separation for BC tracer tagging. Red circle indicates location of Syowa Station, Antarctica.

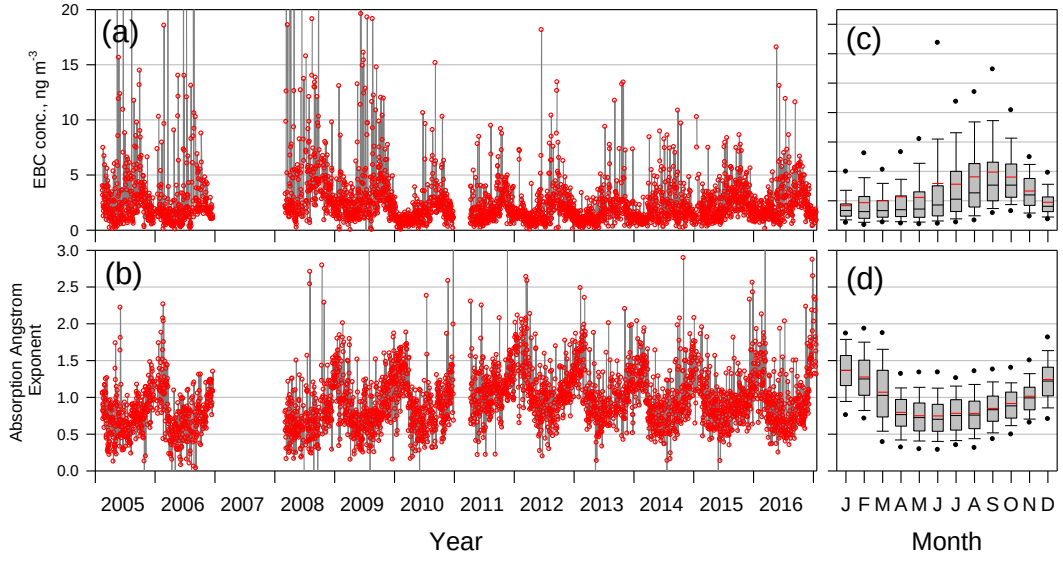

Figure 3: Seasonal features of (a) daily median EBC concentrations, (b) daily median AAE (λ = 370–950 nm), (c) monthly box plot of EBC concentrations, and (d) monthly box plot of AAE at Syowa since February 2005. EBC concentrations were not available in Jan. 2007 – Jan. 2008 and January 2011 – early April 2011 because of mechanical trouble in the aethalometer. Blue line in (a) shows the detection limit (0.2 ng m^{-3}) in our measurements. In box plots, the upper bar, upper box line, black middle box line, bottom box line, and bottom bar respectively denote values of 90%, 75%, 50% (median), 25%, and 10%. The red line shows mean values.

Atmos. Chem. Phys. Discuss., https://doi.org/10.5194/acp-2018-1190
Manuscript under review for journal Atmos. Chem. Phys.
Discussion started: 7 January 2019
© Author(s) 2019. CC BY 4.0 License.

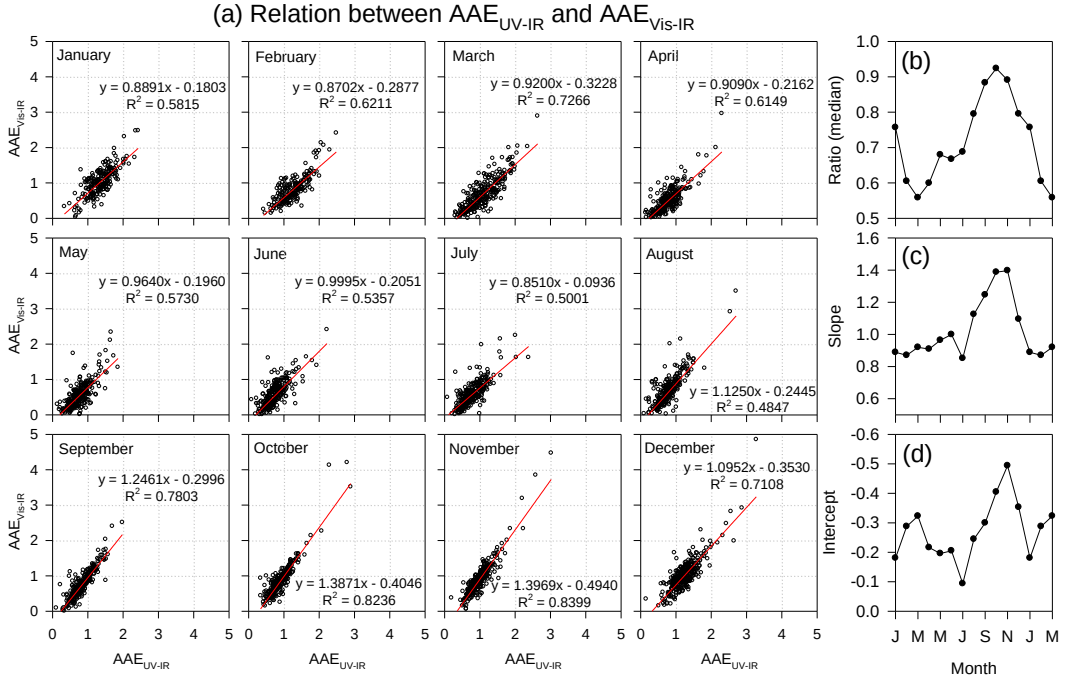

Figure 4: (a) Relations between absorption Angstrom exponent (AAE) in UV-IR channels and AAE in Vis-IR channels, and seasonal features of (b) ratios of $AAE_{Vis-IR}/AAE_{UV/IR}$, and (c) slope and (d) intercepts in the linear regression lines. AAE data with BC concentrations lower than 0.2 ng m^{-3} (detection limit) were excluded from the plots. Red lines represent regression lines.

Atmos. Chem. Phys. Discuss., https://doi.org/10.5194/acp-2018-1190
Manuscript under review for journal Atmos. Chem. Phys.
Discussion started: 7 January 2019
© Author(s) 2019. CC BY 4.0 License.

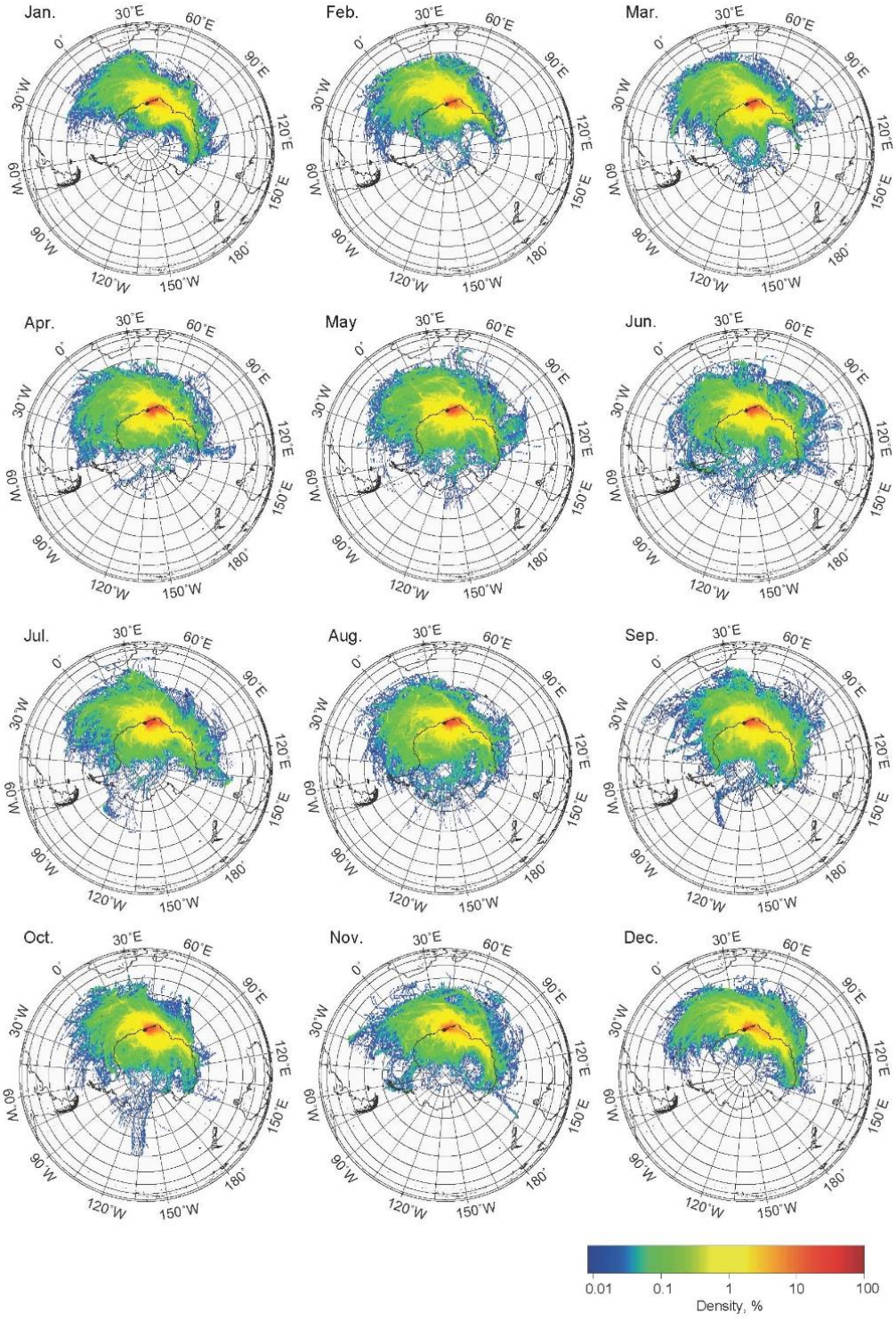

Figure 5: Density map of air mass origins in each month at Syowa Station. Black points denote the respective locations of Syowa Station.

Atmos. Chem. Phys. Discuss., https://doi.org/10.5194/acp-2018-1190
Manuscript under review for journal Atmos. Chem. Phys.
Discussion started: 7 January 2019
© Author(s) 2019. CC BY 4.0 License.

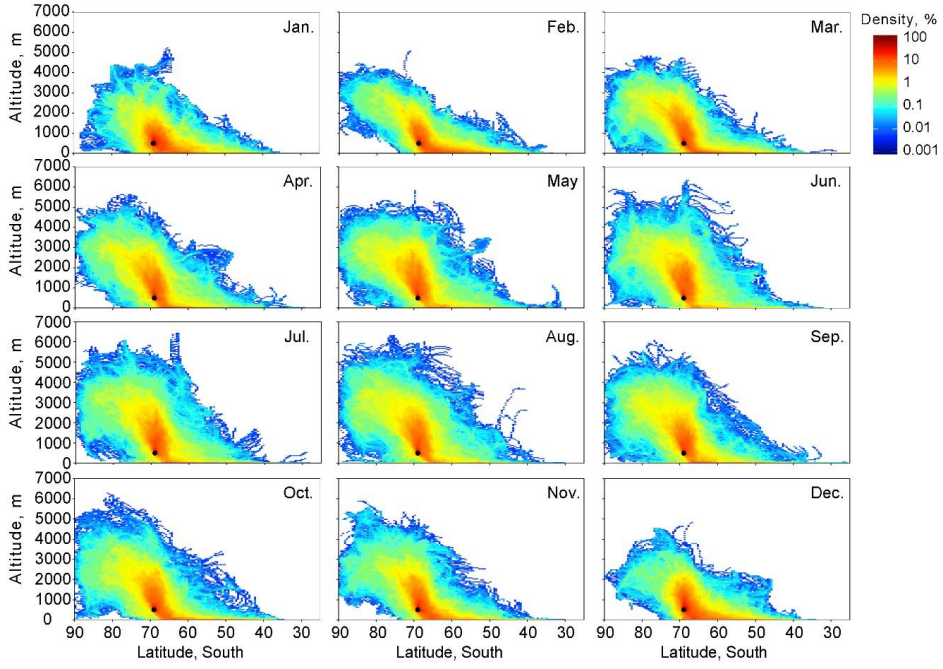

Figure 6: Density plots of vertical motion of air masses transported to Syowa Station in each month. Black points show initial points of the trajectory analysis over Syowa Station. Altitudes denote "above ground level".

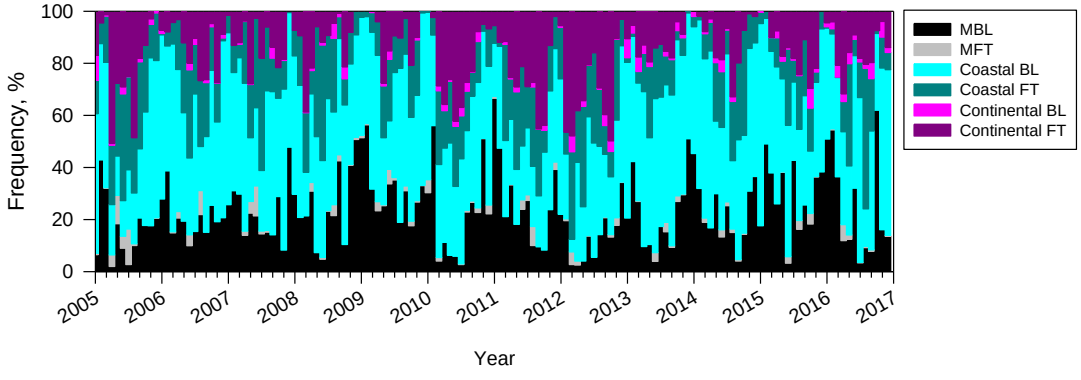

Figure 7: Seasonal features of air mass origins at Syowa Station. MBL, MFT, coastal BL, coastal FT, continental BL, and continental FT respectively denote the marine boundary layer, marine free troposphere, coastal boundary layer, coastal free troposphere, continental boundary layer, and continental free troposphere.

Atmos. Chem. Phys. Discuss., https://doi.org/10.5194/acp-2018-1190
Manuscript under review for journal Atmos. Chem. Phys.
Discussion started: 7 January 2019
© Author(s) 2019. CC BY 4.0 License.

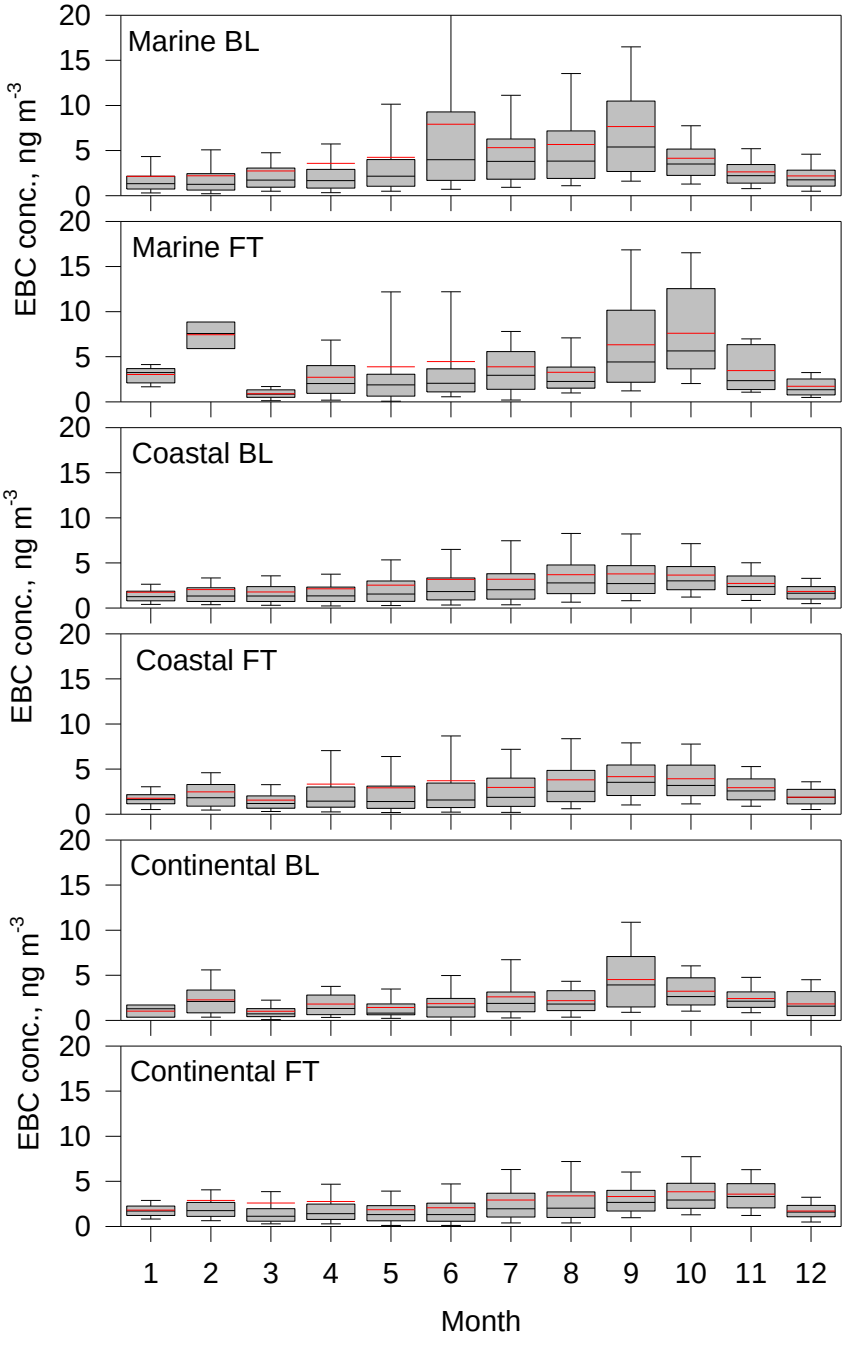

Figure 8: Seasonal features of hourly mean EBC concentrations in each air mass origin at Syowa Station. MBL, MFT, coastal BL, coastal FT, continental BL, and continental FT respectively denote the marine boundary layer, marine free troposphere, coastal boundary layer, coastal free troposphere, continental boundary layer, and continental free troposphere. In box plots, the upper bar, upper box line, black middle box line, bottom box line, and bottom bar respectively denote values of 90%, 75%, 50% (median), 25%, and 10%. The red line represents mean values.

Atmos. Chem. Phys. Discuss., https://doi.org/10.5194/acp-2018-1190
Manuscript under review for journal Atmos. Chem. Phys.
Discussion started: 7 January 2019
© Author(s) 2019. CC BY 4.0 License.

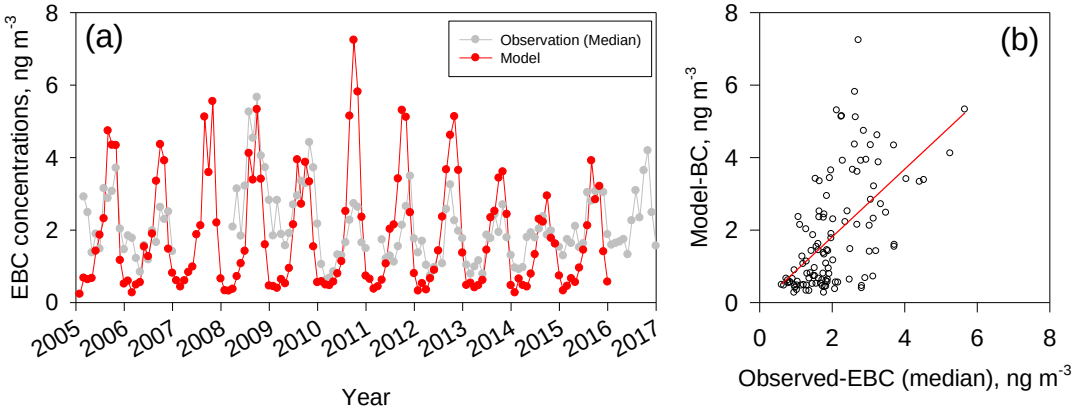

Figure 9: (a) Seasonal features of monthly median EBC concentrations and model-BC concentrations at Syowa Station and (b) the relation between monthly median EBC concentrations and model-BC concentrations. The red line in (b) shows the regression line.

Atmos. Chem. Phys. Discuss., https://doi.org/10.5194/acp-2018-1190
Manuscript under review for journal Atmos. Chem. Phys.
Discussion started: 7 January 2019
© Author(s) 2019. CC BY 4.0 License.

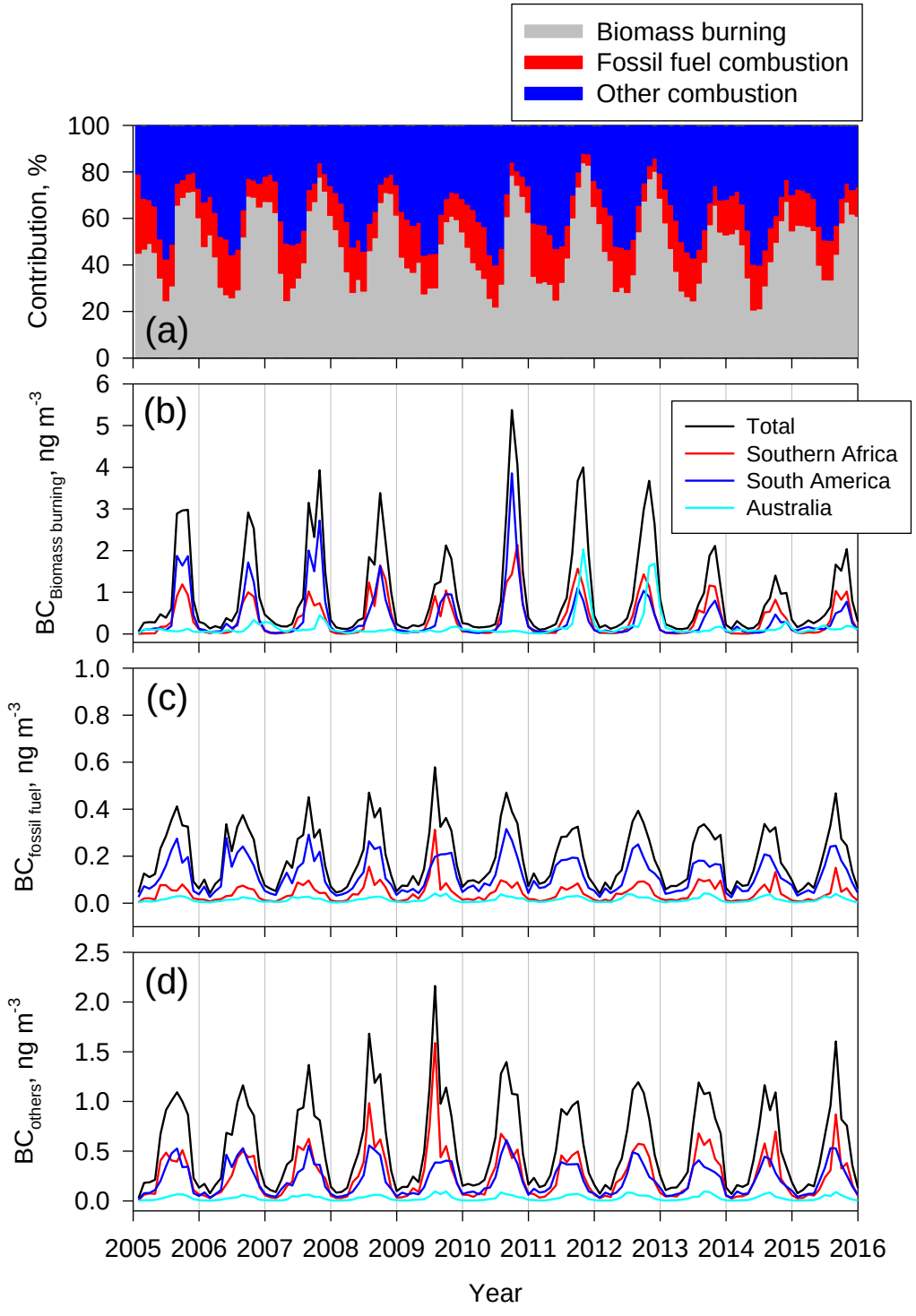

Figure 10: Seasonal features of (a) contribution of potential origins of BC transported to Syowa Station, (b) the concentrations of BC released from biomass burning, (c) the concentrations of BC released from combustion of fossil fuels, and (d) the concentrations of BC released from the other origins in the model simulation.